Development of a Magnetically-Suspended Mirror Scanning Mechanism for an Interferometric Monitor for Greenhouse Gasses (IMG)

T. AKIBA, S. SHINGU, Y. KAMEDA, S. AKABANE AND S. HIRAI

ABSTRACT

The Advanced Earth Observation Satellite (ADEOS) will be launched in early 1995. It carries an Interferometric Monitor for Greenhouse gasses (IMG). The IMG program has been implemented under the contract for " An assessment of the environment (A study of the global monitoring)" of the Ministry of International Trade and Industry since 1989.

IMG is intended for the global observation of CO_2, CH_4, N_2O and other greenhouse effect gasses. It is a fourier transform infrared spectrophotometer (FTIR) , and requires a scanning mirror and the mirror scanning mechanism for fourier transform.

In the IMG system, the mirror scanning mechanism is a key part. Accordingly, the authors manufactured the Magnetically–Suspended Mirror Scanning Mechanism (MAMS) for IMG. This paper presents the MAMS structure and the results obtained from its functional tests.

INTRODUCTION

The Advanced Earth Observation Satellite (ADEOS) will be launched for global observation of the earth environment. It will be placed into a sun synchronous orbit. Observations from space bring global atmospheric information.

In our earth atmosphere, there are many ingredients such as carbon–dioxide, methane and nitrogen–dioxide. They absorb outgoing infrared radiation from the Earth to the space and warm up the Earth atmosphere, in the so–called " Greenhouse effect" . Recent human activity increases such greenhouse gasses, and the increase in the temperature of the atmosphere is predicted to be 0.3 deg. within this century.(Ref.[1])

The Interferometric Monitor for Greenhouse gasses (IMG) is intended to be used for global investigation on the greenhouse effect,

Toshikatsu Akiba, Shitta Shingu, Toshiba Corporation R&D Center,
4–1 Ukishima–cho,Kawasaki–ku,Kawasaki,210,Japan
Yoshihiko Kameda,Satoshi Akabane,Toshiba Corporation,Komukai Works,
1 KomukaiToshiba–cho,Saiwai–ku, Kawasaki,210,Japan
Shoichi Hirai,Japan Resources Observation System Organization,
3–15–3 Nishi–Shimbashi,Minato–ku,Tokyo,105, Japan

the amount of greenhouse gasses, air pollution and gaseous exchange between the troposphere and lower stratosphere.

IMG is a fourier transform infrared spectrophotometer (FTIR). It needs a scanning mirror driving mechanism with high directional accuracy.

The authors developed a Magnetically–suspended Mirror Scanning Mechanism (MAMS) for IMG, which advantages are high directional accuracy during scanning. This paper presents the MAMS structure and the results of its functional tests.

IMG OPTICS

IMG is an FTIR using a Michelson interferometer scheme. The main optical components are the Image Motion Compensation Mirror (IMCM), the fixed mirror, the scanning mirror, the beam splitter and some detectors. Figure 1 shows the optical layout for IMG. IMCM compensates the field of view during IMG measurement.

In the FTIR system, the mirror scanning mechanism is a key part, which has great influence on the sensor performance. For example, the

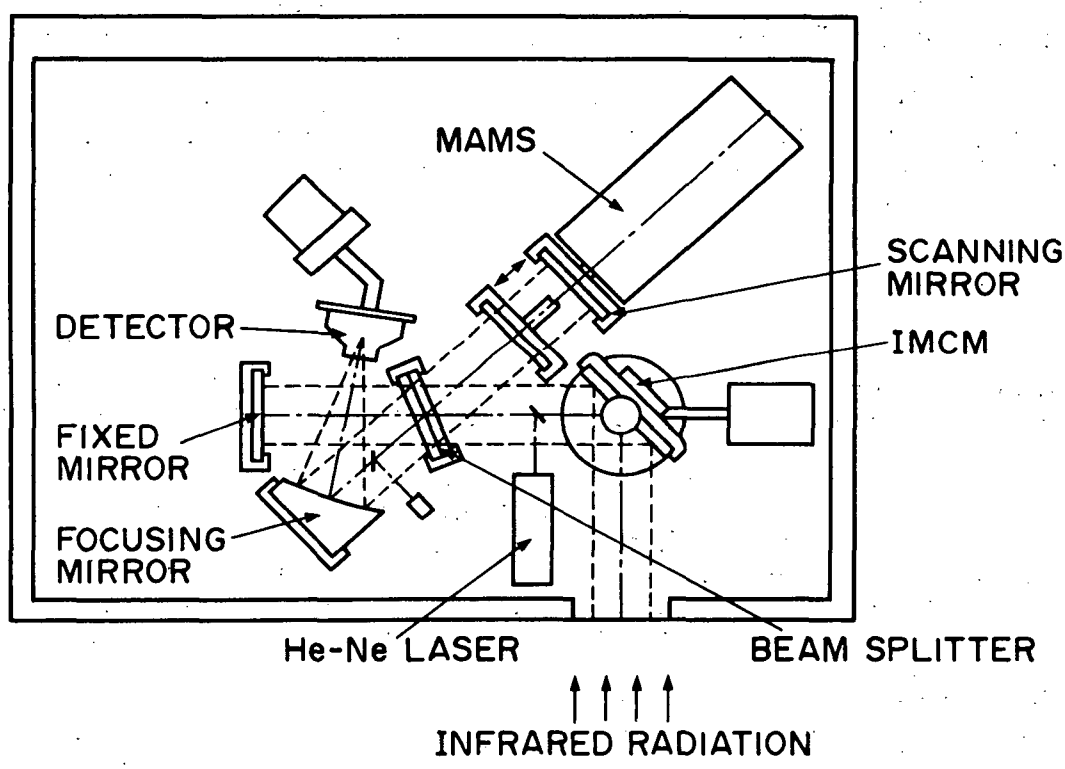

Figure 1. IMG OPTICAL LAYOUT

scanning mirror moving stroke decides the sensor resolution, thus the resolution will become finer as the scanning stroke becomes longer. The modulation efficiency is raised with the higher scanning mirror directional accuracy. Therefore, it is necessary for the high IMG sensor performance that MAMS has a long scanning stroke and excellent directional accuracy.

MIRROR SCANNING SYSTEM DESIGN

REQUIREMENTS

The IMG system requires that MAMS has long stroke and excellent directional accuracy. The required specifications for MAMS are as follows.

1. The scanning mirror should be controlled with an excellent directional accuracy, on the order of 0.0001 degrees.
2. The scanning mirror has to move 50 mm around the zero path difference position, so the scanning stroke is 100 mm long.
3. The interferogram acquisition time is 10 seconds. Thus, the scanning speed is 10 mm/sec.
4. The mechanism mass is less than 10 kg.

MECHANISM

Many other researchers developed the transporting mechanism, such as Ota, et al.[2] and Hanel, et al.[3]. The authors took on a magnetic bearings and linear motor type mirror scanning mechanism, which has such advantages as simple structure, high directional accuracy, and non–contact drive. Therefore, it has no friction, no wear, no lubrication required and has excellent mechanism reliability. (Ref.[4],[5],[6])

Figure 2 shows MAMS view for IMG, and Fig. 3 shows a cross sectional view of MAMS. Main MAMS components are a scanning mirror, a scanning mirror shaft made of ferromagnetic material (the floating shaft), two magnetic bearings, a linear motor for the mirror scanning motion, nine eddy current displacement sensors and several support members. In the six degrees of freedom for the motion, the magnetic bearings for MAMS actively control the four axes. These are two displacements, perpendicular to the scanning axis, and two tiltings for the scanning mirror shaft. The rotation around the scanning axis is passively stabilized. The motion along the scanning axis is driven by the linear motor. A magnetic bearing has two actuators. Each actuator consists of a pair of electromagnets, opposite to each other. The linear motor for the mirror scanning motion is a moving magnet linear–actuator.

The sensor targets on the floating shaft are used for detecting the shaft position. These sensor targets are separated from magnetic poles. Therefore, the sensor targets have no influence due to the

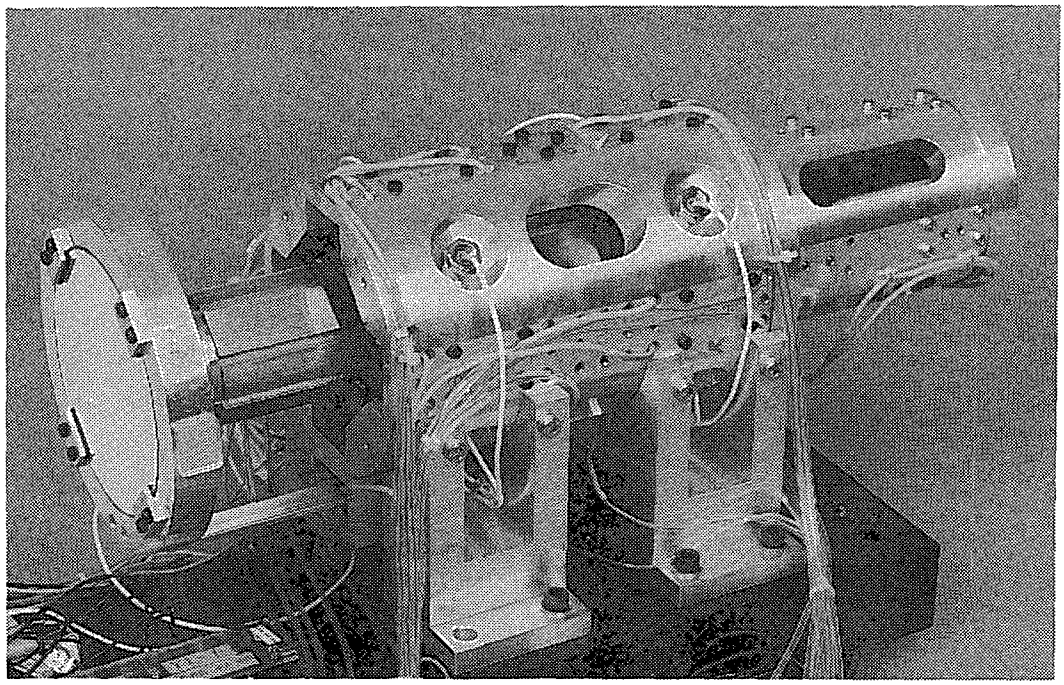

Figure 2. MAMS

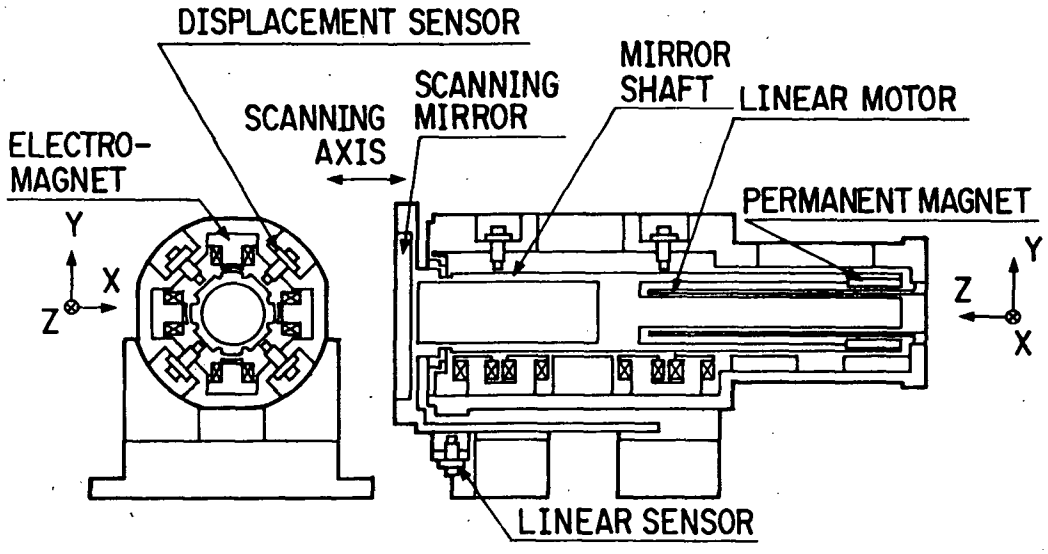

Figure 3. MAMS SCHEMATIC CROSS SECTION

magnetic field from the electromagnets. It is possible to work upon the target with marked flatness, on an order of less than 1μm within the scanning area.

The linear motor consists of a linear motor coil and a permanent magnet fixed in the floating shaft. MAMS is compact, because the linear motor coil is interposed in the shaft. The permanent magnetic flux for the linear motor passes down the working air gap, axially along the floating shaft, then returns to the permanent magnet. The electromagnetic flux in the air gaps for the magnetic bearing has no influence from the permanent magnetic flux in the linear motor, because the electromagnet circuits are closed locally. The permanent magnet flux, that passes the air gap in the electromagnet circuit, is almost zero. The outstanding MAMS features are as follows.

1. The floating shaft is suspended by eight electromagnets, so MAMS is a non–contact supporting mechanism.
2. The magnetic bearings in MAMS actively control the four axes.
3. All bias flux and all control flux are generated by the electromagnets.
4. The sensor targets are completely isolated from the magnet field of the electromagnets.

The specifications for MAMS are shown in Table I.

MAMS is a bread board model. Therefore, MAMS does not have a special equipment suited to space environment, for example a launch lock device. However these technologies are already established, so MAMS can easily be converted into a flight model.

TABLE I SPECIFICATIONS

ITEMS	CHARACTERISTICS
DEGREES OF FREEDOM (CONTROLLED)	5
POINTING RANGE	±0.1 deg.
SCANNING MIRROR DIAMETER	110 mm
FLOATING SHAFT MASS	2.72 kg
TOTAL MASS	7.6 kg
TOTAL SIZE	180×330×180 mm

DYNAMICS

OPEN LOOP STIFFNESS AND ACTUATOR GAIN

There is no coupling between the X axis forces and the Y axis forces, because the floating shaft shape is simple and each force axis is perpendicular to the other in a small moving range.

The force generated by a magnetic bearing on a suspended shaft in its field is a function of the geometry of the magnetic circuit and magnetic inductance in working air gaps. MAMS's geometry is very simple. In this geometry, where a floating shaft is suspended between two opposing electromagnets using current control, the magnetic forces are given by the following well known expression.(Fig.3)

$$F=k\{(Ib+Ic)^2/(Lg+x)^2-(Ib-Ic)^2/(Lg-x)^2\} \quad (1)$$

where constant k depends on the bearing design parameters, Ib is bias current, Ic is the control current, Lg is the nominal air gap and x is the shaft displacement from the unstable nominal equilibrium position.

For studying the dynamic performance of the closed loop system, a linearized actuator mathematical model of the magnetic bearing is required. So, the magnetic forces can be written as a linearized equation at x=0, as follows.

$$F = df/dx|_{x=0} \times \Delta x + df/di|_{x=0} \times \Delta i \quad (2)$$

The bearing forces for MAMS are given by Eq.(2) and the MAMS design parameters.

$$F=kx\times\Delta x+ki\times\Delta i \quad (3)$$

$$=-5.6\times10^4\times\Delta x+27.3\times\Delta i$$

The linearized actuator properties are identified from Eqs.(2) and (3), as

$$kx=df/dx \quad \text{and} \quad ki=df/di \quad (4)$$

The constant kx can be described as stiffness. The stiffness of the support is governed by kx in the absence of a feedback loop, so this term is referred to as the open loop stiffness. The constant kx is negative, indicating the open loop instability of the magnetic bearing. The constant ki relates the actuator force to the control current, so it is called the actuator gain.

CONTROLLER

Figure 4 shows a blockdiagram for the magnetic suspension control system. The displacement between the floating shaft and the sensor is detected by the displacement sensor. The sensor signal is transformed into the displacement from the nominal equilibrium position of floating shaft. The actuator consisting of two opposing electromagnets is independently controlled by an individual analog PID controller according to the displacement signal.

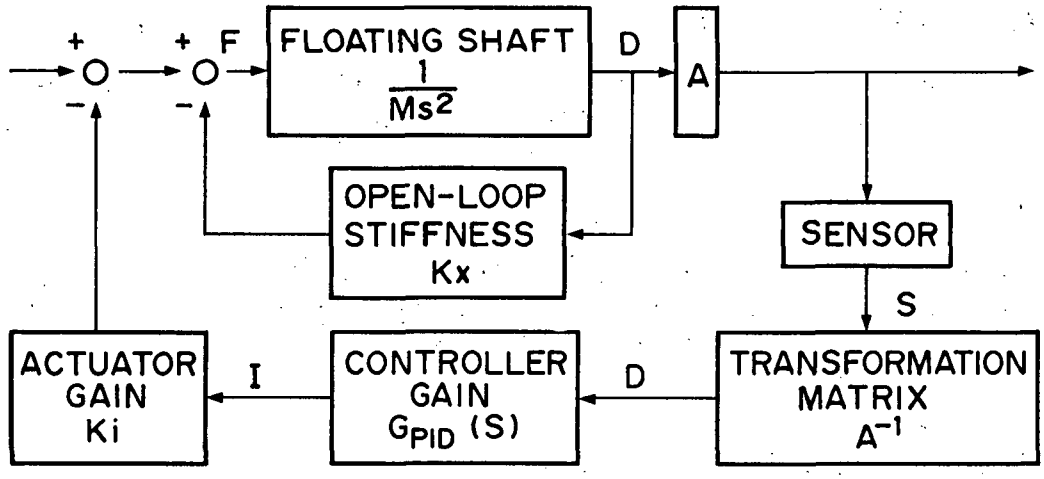

Figure 4. MAMS CONTROL BLOCKDIAGRAM

POSITION TRANSFORMATION

The sensor signals of the floating shaft position described as a function of x,y and θz, including the rolling effect of the shaft. It is as follows.

$$S=f(x,y,\theta z) \tag{5}$$

Applying the linear approximation at the nominal equilibrium position to Eq.(5), the relationship is obtained as follows.

$$\Delta S=A\times\Delta D \tag{6}$$

Where the matrix **A** is the transformation matrix decided by the MAMS housing shape with the displacement sensors. ΔD is the displacement vector of the floating shaft. ΔS is sensor signal vector. Therefore, ΔD is obtained as follows.

$$\Delta D=A^{-1}\times\Delta S \tag{7}$$

where the matrix A^{-1} is the transformation matrix from the sensor signals to the floating shaft displacement. The matrix A^{-1} is materialized by electric circuits.

The floating shaft displacement in the direct motion can be calculated from Eq.(7). Therefore, one magnetic bearing actuator can be independently controlled by one PID controller.

EXPERIMENTAL RESULTS

MAMS's characteristics are shown in Table Ⅱ. These experiments were carried out in atmosphere at room temperature.

SCANNING STROKE

The scanning mirror shaft is suspended by the magnetic suspension. It is moved from the starting position of the scanning motion to the ending position. The scanning stroke is confirmed as being 119 mm long.

STATIC DIRECTIONAL ACCURACY

When pointing the scanning mirror at any point on the scanning axis, the static directional error for the scanning mirror was determined by means of an autocollimator. As the test results showed, the static directional accuracy on the X–axis was confirmed to be 0.000048 deg.(1σ). Similarly, the accuracy on the Y–axis was confirmed to be 0.000073 deg.(1σ). This static directional error is caused by the error in the control loop, including the PID controller, the current driver, the sensor error and the sensor target surface roughness.

TABLE Ⅱ PERFORMANCE

ITEMS	PERFORMANCE	
STROKE	119	mm
STATIC ACCURACY (1σ)		
on X-axis	4.8×10^{-5}	deg.
on Y-axis	7.3×10^{-5}	deg.
DYNAMIC ACCURACY (1σ)		
on X-axis	1.9×10^{-4}	deg.
on Y-axis	3.4×10^{-4}	deg.
POINTING LINEARITY		
on X-axis	1.45	%
on Y-axis	2.35	%

DYNAMIC DIRECTIONAL ACCURACY

When scanning the mirror along the scanning axis, the directional error during the scanning motion was determined in the same way. This is called dynamic directional accuracy. As a result of the tests, the dynamic directional accuracy on the X−axis was confirmed to be 0.00019 deg.(1σ). Similarly, the dynamic directional accuracy on the Y−axis was confirmed to be 0.00034 deg.(1σ). Figure 5 shows the X−axis accuracy. This directional error on the X−axis is mainly caused by the sensor target flatness within the scanning area. The directional error on the Y−axis is influenced by gravity. However, the directional accuracy in orbit can be estimated by the X−axis accuracy.

POINTING MOTION

MAMS provides the ability to re−align the scanning mirror. The pointing linearity was confirmed by pointing tests. Figures 6 shows the test result on the X−axis. The pointing linearity on the X−axis is 1.45% for the test range(0.18 deg.). Similarly, the pointing linearity on the Y−axis is 2.35% for the test range(0.15 deg.).

CONCLUSIONS

A mirror scanning mechanism for IMG, using magnetic suspension and linear motor, was developed. Its scanning motion characteristics were clearly confirmed to be allowable by several experiments. MAMS's advantages, realized in the manufactured mechanism, are as follows.

(a) Dynamic accuracy during scanning motion is 0.00019 deg.(1σ) on the X−axis. This represents the accuracy under no gravity condition.
(b) MAMS provides the ability for re−aligning the scanning mirror.
(c) Simple construction and excellent dynamic directional accuracy were achieved with no friction, no wear and no lubrication required.

REFERENCES

1. Tsuno, K., Y. Kameda, K. Kondoh, S. Hirai, 1991. " Interferometric monitor for greenhouse gasses for ADEOS." , SPIE, Vol.1490, " Future European and Japanese Remote Sensing Sensors and Programs" , 222−232.
2. Ota, M., S. Andoh, H. Inoue, 1990. " MAG−LEV SEMICONDUCTOR WAFER TRANSPORTER FOR ULTRA−HIGH−VACUUM ENVIRONMENT (Application Development of Active Magnetic Bearing)." , Proceedings of the second International Symposium on Magnetic Bearings, 109−114.
3. Hanel, R.A., B. Schlachman, D. Rogers, and D. Vanous, 1971. " Nimbus 4 Michelson Interferometer." , APPLIED OPTICS, Vol.10, No.6, 1376−1382.

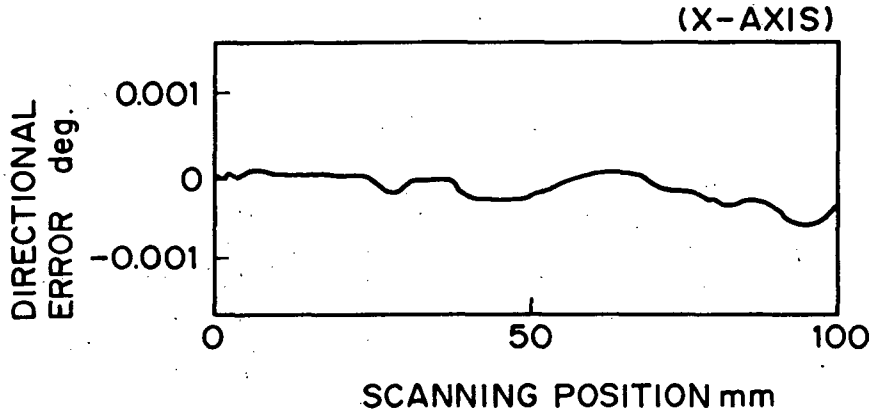

Figure 5. DYNAMIC DIRECTIONAL ACCURACY

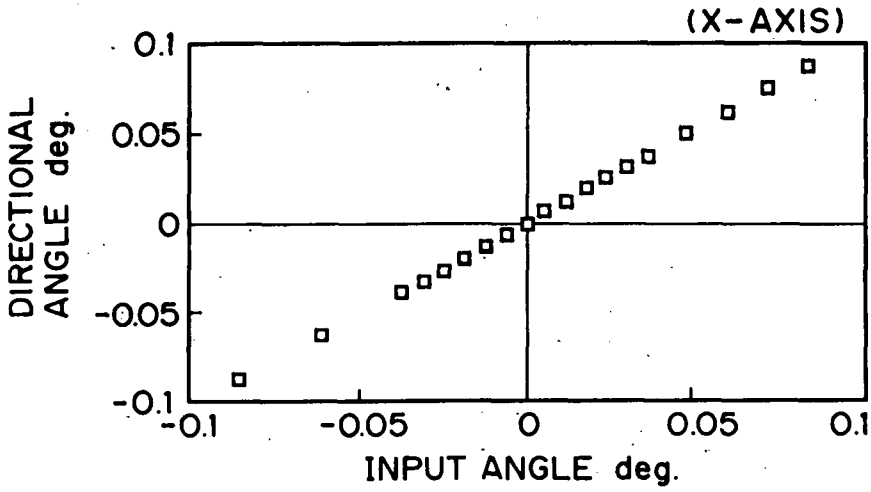

Figure 6. POINTING MOTION

4. Takahara, K., T. Ozawa, H. Takahashi, S. Shingu, T. Ohashi, H.Sugiura, 1988. " DEVELOPMENT OF A MAGNETICALLY SUSPENDED TETRAHEDRON–SHAPED ANTENNA POINTING SYSTEM." , Proceedings of 22nd Aerospace Mechanisms Symposium, 133–147.
5. Sortore, C.K., P.E. Allaire, E.H. Maslen, R.R. Humphric, P.A. Studer, 1990. " PERMANENT MAGNET BIASED MAGNETIC BEARINGS–DESIGN, CONSTRUCTION AND TESTING." , Proceedings of the second International Symposium on Magnetic Bearings, 175–182.
6. Siegwart, R., R. Larsonneur, A. Traxler, 1990. " DESIGN AND PERFORMANCE OF A HIGH SPEED MILLING SPINDLE IN DIGITALLY CONTROLLED ACTIVE MAGNETIC BEARINGS." ,Proceedings of the second International Symposium on Magnetic Bearings, 197–204.